Макрогетероциклы
http://mhc-isuct.ru

DOI: 10.6060/mhc235121m

Characterizing the Conformational Behavior of Yttrium(III) Tris-Phthalocyaninates Using Variable Temperature NMR Spectroscopy

Alexander G. Martynov,[a@] and Gayane A. Kirakosyan[a,b]

[a]*Frumkin Institute of Physical Chemistry and Electrochemistry, Russian Academy of Sciences, 119071 Moscow, Russia*
[b]*Kurnakov Institute of General and Inorganic Chemistry, Russian Academy of Sciences, 119991 Moscow, Russia*
[@]*E-mail: martynov@phyche.ac.ru*

Dedicated to Academician Irina P. Beletskaya on the occasion of her Anniversary

We present a variable-temperature NMR study of the conformational behavior of homo- and heteroleptic yttrium(III) triple-decker complexes containing butoxy- and 15-crown-5-substituted phthalocyanine ligands ***Y_2[(BuO)$_8$Pc]$_3$*** *and* ***[(BuO)$_8$Pc]Y[(BuO)$_8$Pc]Y[(15C5)$_4$Pc]*** *in dichloromethane. In the homoleptic complex, the adjacent BuO-substituted ligands form gauche conformers, which undergo interconversion due to rapid rotation around the C_4 axis. In contrast, in the heteroleptic complex, the inner BuO- and the outer 15C5-substituted ligands are in the staggered conformation; moreover, such an arrangement of the ligands has been shown to decrease the rotation rate of the outer BuO-substituted ligand. This allowed to find the coalescence temperature (223 K) and to determine the activation energy E_A (57.7±3.4 kJ/mol) and other thermodynamic properties of the ligand rotation in the heteroleptic complex. These conclusions were supported by DFT GIAO calculations. The obtained results will be useful for further characterization of magnetic properties of paramagnetic analogues of the synthesized complexes using VT-NMR spectroscopy.*

Keywords: Triple-decker complex, phthalocyanine, variable temperature NMR, GIAO approximation, conformation, intramolecular rotation.

Исследование конформационного поведения трисфталоцианинатов иттрия(III) с использованием спектроскопии ЯМР при переменной температуре

А. Г. Мартынов,[a@] Г. А. Киракосян[a,b]

[a]*Институт физической химии и электрохимии им. А.Н. Фрумкина РАН, 119071 Москва, Россия*
[b]*Институт общей и неорганической химии им Н.С. Курнакова РАН, 119991 Москва, Россия*
[@]*E-mail: martynov@phyche.ac.ru*

С использованием спектроскопии ЯМР при переменной температуре проведено исследование конформационного поведения гомо- и гетеролептических трехпалубных комплексов иттрия(III), содержащих бутокси- и 15-краун-5-замещенные фталоцианиновые лиганды ***Y_2[(BuO)$_8$Pc]$_3$*** *и* ***[(BuO)$_8$Pc]Y[(BuO)$_8$Pc]Y[(15C5)$_4$Pc]*** *в дихлорметане. В этих комплексах соседние BuO-замещенные лиганды находятся в скошенных конформациях, переходящих друг в друга за счет быстрого вращения лигандов вокруг оси симметрии C_4. В гетеролептическом комплексе внутренний BuO- и внешний 15C5-замещенный лиганды находятся в заторможенной конформации, и было показано, что такое расположение макроциклов уменьшает скорость вращения внешнего BuO-замещенного лиганда. Это позволило найти температуру коалесценции (223 K) и определить энергию активации E_A (57.7±3.4 кДж/моль) и другие термодинамические характеристики вращения фталоцианинового лиганда в гетеролептическом комплексе. Полученные выводы были подтверждены расчетами с использованием теории функционала плотности в приближении GIAO. Результаты работы будут полезны для дальнейшей характеризации магнитных свойств парамагнитных аналогов синтезированных комплексов с помощью спектроскопии ЯМР.*

Ключевые слова: Трехпалубный комплекс, фталоцианин, ЯМР при переменной температуре, приближение GIAO, конформация, внутримолекулярное вращение.

Introduction

Controlling molecular motion is the key to the development of molecular machines, which are expected to form the basis of future advanced nanotechnologies.[1] Typically, two types of such motion are considered – either gliding of molecular components with respect to each other,[2] or rotation of components around certain axes.[3] The interest in molecular rotation has led to elaboration of various rotors, toppers, brakes, turnstiles, propellers, and gears.

Sandwich complexes with macrocyclic ligands are among the most prominent components of molecular rotors, where rotation occurs around the coordinating metal center.[4,5] For example, this principle guided the design of allosteric receptors based on μ-oxo-diiron(III)[6] and cerium(IV)[7] bisporphyrinates for the recognition of chiral molecules. Another example is the family of heteroleptic crown-substituted trisphthalocyaninates **[(15C5)$_4$Pc]M*[(15C5)$_4$Pc]M(Pc)** (M, M* = Tb, Y), which can bind potassium cations via their intercalation between the crown-ether rings of the adjacent decks.[8] This switches the twist angle between the crown-substituted ligands from 45 to 0°, which affects the symmetry of the coordination polyhedron of the M* metal center. When the paramagnetic Tb^{III} cation is inserted into this site, the axial component of the magnetic susceptibility tensor is greatly enhanced, which is important for the design of magnetic materials.[9,10]

Analogous enhancement of axial anisotropy was observed for heteroleptic **[(BuO)$_8$Pc]M[(BuO)$_8$Pc]M*[(15C5)$_4$Pc]** (M, M* = Tb, Y) complexes – their fragments "M[(BuO)$_8$Pc]$_2$" switched between the staggered and gauche conformations upon changing the solvent from aromatic toluene to aliphatic dichloromethane and chloroform.[11] In contrast, the "[(BuO)$_8$Pc]M*[(15C5)$_4$Pc]" fragment was conformationally invariant and remained in the staggered form in both types of solvents. This behavior was explained by the stabilization of certain conformers by specific solvation, including the formation of hydrogen bonds with crown-ether substituents which blocked the arrangement of the neighboring ligand. Detailed analysis of NMR evidenced that X-ray structural data can be safely extrapolated to the behavior in solutions.

In the present work, we aimed to gain deeper insight into the rotational behavior of the triple-decker complex **[(BuO)$_8$Pc]Y[(BuO)$_8$Pc]Y[(15C5)$_4$Pc]** (Figure 1a) by means of variable temperature ^{1}H NMR spectroscopy.

Results and Discussion

For brevity, the butoxy- and crown-substituted ligands are henceforth referred to as **[B$_4$]** and **[C$_4$]**, where the letters "B" and "C" stand for BuO- and 15C5-substituted phthalic units in the phthalocyanine rings, respectively, so that in this notation the target complexes will be referred to as **[B$_4$]Y[B$_4$]Y[C$_4$]**.

The interest in a detailed characterization of the rotational dynamics of **[B$_4$]Y[B$_4$]Y[C$_4$]** has arisen first of all from the discrepancy between its UV-vis and ^{1}H NMR spectra in halogenated alkanes. For example, the UV-vis spectrum of the title compound in dichloromethane shows the strongly broadened Q-band with multiple inflexions on both the short and long wavelength sides (Figure 1b), which is typical for sandwich complexes existing in gauche conformations in solution.[12,13] In contrast, the ^{1}H NMR spectrum in CD_2Cl_2 demonstrates that all aromatic protons of each type of phthalocyanine ligand are equivalent; *i.e.*, the complex molecules turns out to be highly symmetric (Figure 1c). This contradicts the distorted shape of the molecule, where four aromatic protons of the outer BuO-substituted ligand are expected to be located above the benzene rings of the inner ligand and vice versa (Figure 1d,e), which should result in their shielding with respect to the other four protons that are located above the gap between the benzene rings.

The apparent symmetrization of the ^{1}H NMR spectrum could result from the exchange between two gauche conformers due to the fast rotation of the ligands around the C_4 symmetry axis (Figure 1c). Therefore, we used variable temperature NMR spectroscopy in the range of 293–193 K to see if the rotation could be slowed down on the NMR time scale and determine its thermodynamic characteristics

Indeed, cooling the sample resulted in a gradual broadening of the resonance signals of the aromatic protons of the butoxy-substituted ligands bH_{Pc}^{o} and bH_{Pc}^{o}, with their disappearance at 223 K (Figure 2a). Further cooling resulted in the appearance of four signals whose shapes and positions stabilized by reaching the temperature of 193 K. The maximum separation δν between the pairs of exchanging resonances corresponding to the outer and inner BuO-substituted decks achieved at low-temperatures was 517 and 665 Hz, respectively.

In contrast, the broadening of the resonance signal of cH_{Pc}^{o} was much less pronounced and its signal was observed in the whole temperature range. Overall, the spectra below 213 K corresponded to those expected for the molecule in which the [B$_4$]Y[B$_4$] fragment is in the gauche conformation and [B$_4$]Y[C$_4$] is in the staggered form.

These results are in general agreement with DFT calculations (Figure 2b) performed to estimate the chemical shifts of aromatic protons in the model complex **Y$_2$[M$_4$]$_3$**, where two pairs of adjacent octamethoxy-substituted phthalocyanine ligands are in staggered and gauche conformations (Figure 3). This model was constructed from the X-ray data for the solvate **[B$_4$]Y[B$_4$]Y[C$_4$]·10CH$_2$Cl$_2$** by removing the solvate molecules, truncating the substituents to leave only methyl groups proximal to the Pc ligands, and optimizing the positions of the hydrogen atoms using the semiempirical PM6-DH2X method[14] on MOPAC2016.[15] This procedure allowed all the structural features of the macrocyclic core to be retained for further calculations.

The isotropic chemical shielding σ for the thus obtained geometry was calculated using the gauge-independent atomic orbital (GIAO)[16] method implemented in the ORCA 5.0.3 package[17] with TPSS functional,[18] pcSseg-2 basis set for light elements[19,20] and LANL2 effective core potential for yttrium,[21] followed by averaging the obtained values for the chemically equivalent protons. The calculation of σ for tetramethylsilane (TMS) was performed at the same level of theory, so subtracting the shielding of the complex protons from σ^{TMS} allowed us to calculate the required chemical shifts, and their comparison with the experiment demonstrated the perfect agreement between these values, assuming certain simplifications of the computational model.

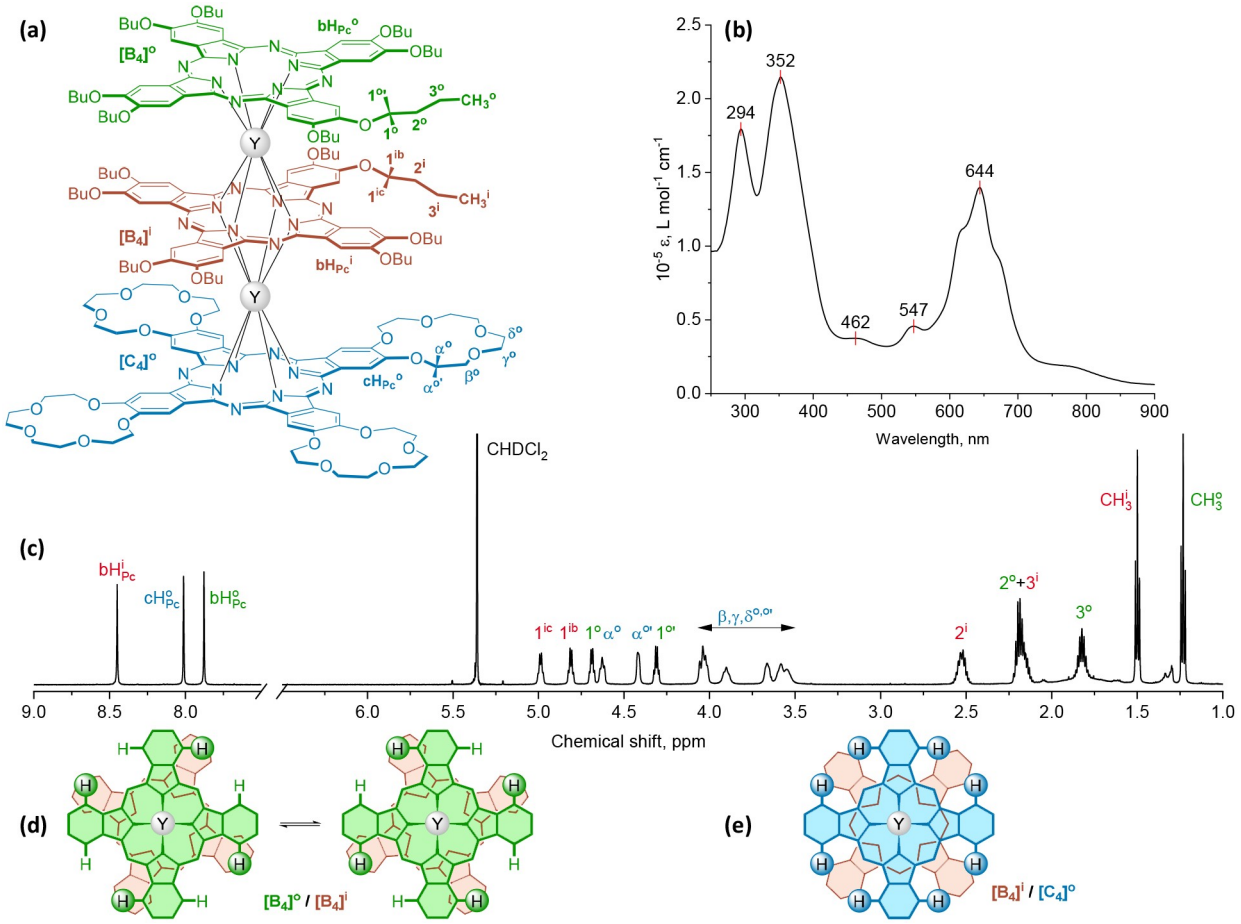

Figure 1. (a) – The heteroleptic trisphthalocyaninate **[B$_4$]Y[B$_4$]Y[C$_4$]** studied here with labeling of the protons used to assign the ^{1}H NMR spectra. (b) – UV-Vis spectrum of the complex in dichloromethane. (c) – ^{1}H NMR spectrum of the complex in CD_2Cl_2 acquired at 293 K. (d) – Top view of the [B$_4$]Y[B$_4$] fragment in the gauche conformation, explaining the difference in the chemical environment of protons located above the underlying benzene ring (highlighted with a green ball) or above the gap between the benzene rings and the exchange between these positions due to switching between the conformers. (e) – Top view of the [B$_4$]Y[C$_4$] fragment in the staggered conformation explaining the equivalence of aromatic protons of the [C$_4$] ligand.

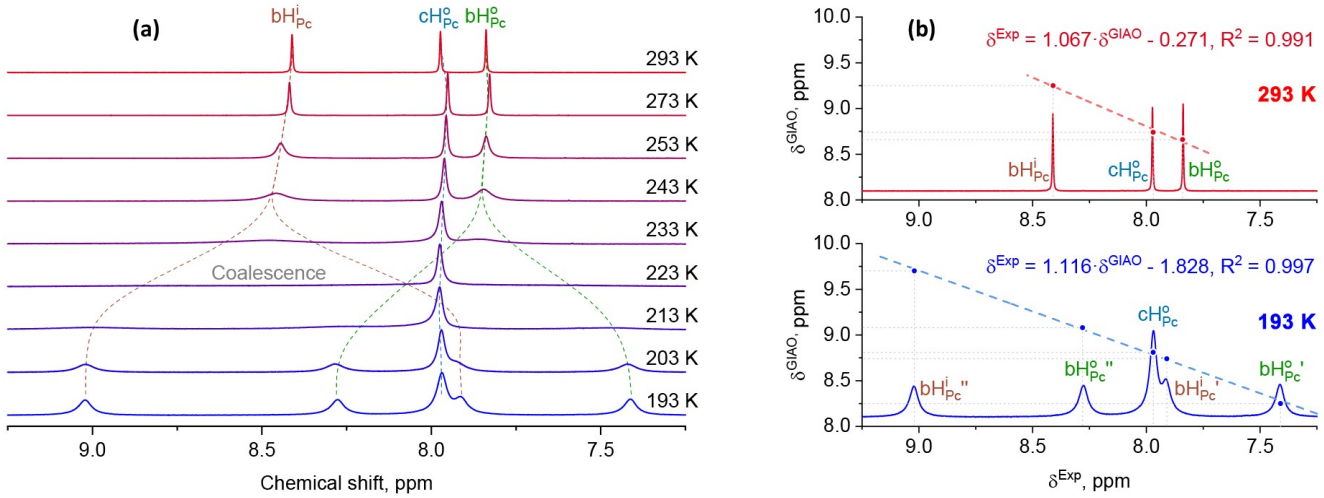

Figure 2. (a) – Evolution of the aromatic part of ^{1}H NMR spectra of **[B$_4$]Y[B$_4$]Y[C$_4$]** in CD_2Cl_2 upon cooling from 293 to 193 K. (b) – Correlation between the experimental ^{1}H NMR spectra of **[B$_4$]Y[B$_4$]Y[C$_4$]** in CD_2Cl_2 at 293 and 193 K and the chemical shifts for the model complex **Y$_2$[M$_4$]$_3$** calculated at the DFT TPSS/pcSseg-2 level using the GIAO method. Dotted lines show the least-squares fits between the calculated δ^{GIAO} and the experimental δ^{Exp} chemical shifts.

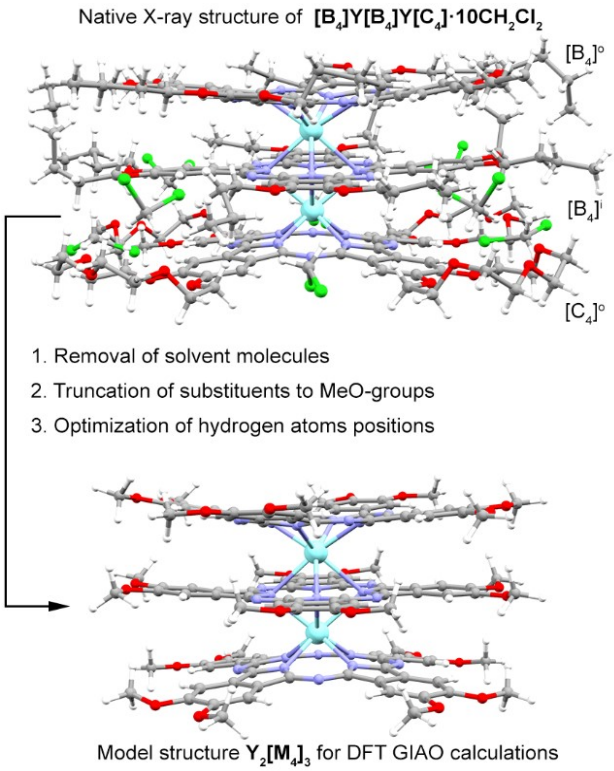

Figure 3. Constructing the model molecule $\mathbf{Y_2[M_4]_3}$ for DFT GIAO calculations.

For the further analysis, the resonance of the outer [B_4] ligand is used as its signals can do not overlap with any other resonances, which facilitates the measurements of their characteristics.

The barrier corresponding to the rotation of the ligands in the [B_4]Y[B_4] fragment was calculated using the Arrhenius dependency of the chemical exchange constant k *vs*. the reciprocal temperature, equation (1):

$$k = k_0 \cdot \exp\left(-\frac{E_A}{RT}\right) \quad (1)$$

Here, T – temperature in K, k_0 – frequency factor, R – universal gas constant (8.31 J mol^{-1} K^{-1}).

The exchange constants were calculated using the well-documented approach[22,23] at the regions of fast exchange [298–233 K, equation (2)], coalescence point [T_c 223 K, equation (3)] and slow exchange [213-193 K, equation (4)]:

$$k_{fast} = \frac{\pi}{2} \cdot \frac{\delta\nu^2}{\Delta_{1/2} - \Delta^f_{1/2}} \quad (2)$$

$$k_c = \frac{\pi}{2}\delta\nu \quad (3)$$

$$k_{slow} = \pi\left(\Delta_{1/2} - \Delta^s_{1/2}\right) \quad (4)$$

Here, δν is the separation between the exchanging resonances at the low temperature limit; $\Delta_{1/2}$ - half-width of the resonance signal at the given temperature, $\Delta^f_{1/2}$ and $\Delta^s_{1/2}$ are half-widths of the resonance signal at the high and low temperature limits. All values are used in Hz.

Thus, plotting ln(*k*) *vs*. 1/T throughout the studied temperature range afforded a straight line with the slope allowing to find the activation energy E_a of 57.7±3.4 kJ/mol (Figure 4a).

Further analysis of the available data was performed using the Eyring equation (5) which allowed to find the free energy of activation $\Delta G^{\neq}$ at the coalescence temperature, equal to 41.1 kJ mol^{-1}.[24] Plotting ln(K/T) *vs*. T^{-1} allowed us to determine its enthalpic (57.1±1.2 kJ/mol) and entropic (71.8±4.7 J mol^{-1} K^{-1}) contributions (Figure 4b).

$$k = \frac{K_B T}{h} \cdot \exp\left(-\frac{\Delta G^{\neq}}{RT}\right) \quad (5)$$

$$\ln\left(\frac{k}{T}\right) = -\frac{\Delta H^{\neq}}{RT} + \left[\frac{\Delta S^{\neq}}{R} - \ln\left(\frac{h}{K_B}\right)\right] \quad (6)$$

Here, K_B and h are Boltzmann and Plank constants, respectively.

Interestingly, the found $\Delta G^{\neq}$ at T_c for the heteroleptic yttrium(III) trisphthalocyaninate perfectly matches the value of $\Delta G^{\neq}$ 40.5 kJ/mol which was previously found for the siloxane dimer (μ-O)[(OctO)$_8$PcSi-OSiMe$_2$tBu]$_2$ also existing in the gauche state in dichloromethane.[25]

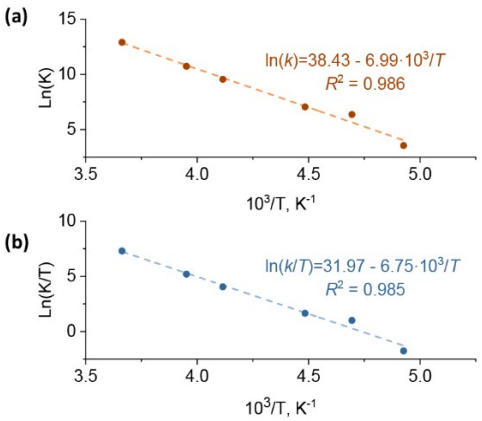

Figure 4. Analysis of VT-NMR data using the logarithmic forms of Arrhenius equation (a) and Eyring equation (b).

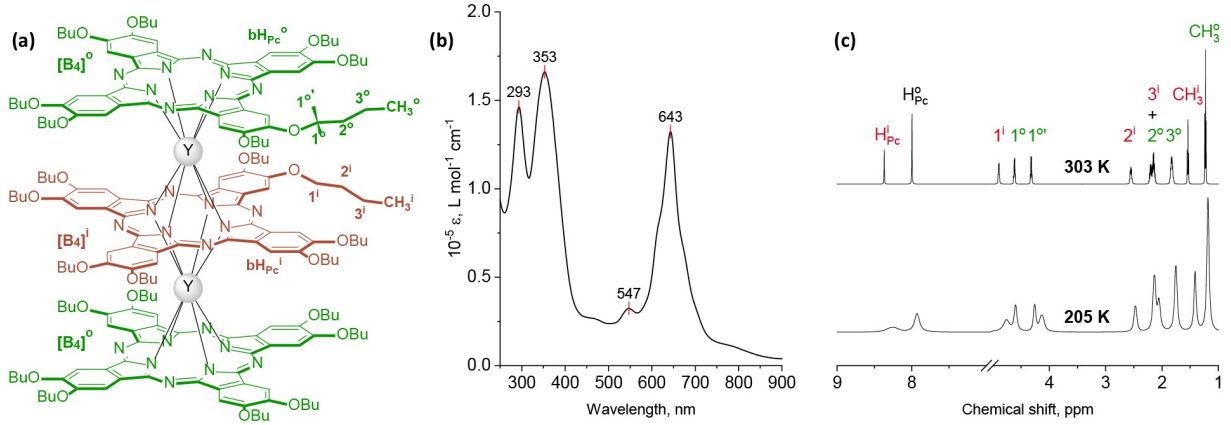

Figure 5. (a) – The homoleptic trisphthalocyaninate $\mathbf{Y_2[B_4]_3}$ studied here, with labeling of the protons used for the assignment of its ^{1}H NMR spectrum. (b) – UV-vis spectrum of the complex in CH_2Cl_2. (c) – VT NMR spectrum of the complex in CD_2Cl_2.

For comparison, we studied the conformational behavior of the homoleptic complex $\mathbf{Y_2[B_4]_3}$, whose UV-vis spectrum also shows that both pairs of adjacent ligands are in gauche conformations (Figure 5).[12] However, no coalescence was observed in the VT NMR spectra of this complex in CD_2Cl_2 upon cooling the sample to 205 K, only a broadening of the signals was observed. Thus, the rotation of the ligands in this complex was fast on the NMR time scale over the entire temperature range.

The analysis of the available X-ray structures of *homoleptic* BuO-substituted triple-deckers $\mathbf{M_2[B_4]_3}$ obtained from dichloromethane solutions (M = Tb,[26] Gd or Gd/Y[27]) is evidence that these complexes do not form any solvates with this solvent; thus, there are no factors which can hinder ligand rotation in the solution state which is in line with the experimental data obtained herein from VT-NMR spectroscopy.

To the contrast, in the *heteroleptic* complex **[B$_4$]Y[B$_4$]Y[C$_4$]** dichloromethane molecules are bound with the 15-crown-5 macrocycles in the crystalline phase, affecting the intramolecular mobility of the inner [B$_4$] ligand (Figure 3);[11] however, the solvate molecules do not interact with the outer [B$_4$] ligand. Thus, we can conclude that complexes of this type can be considered the allosteric receptor where the information about the conformational state of the [B$_4$]Y[C$_4$] site is efficiently transferred to the [B$_4$]Y[B$_4$] site.

Apart from the fundamental interest in the study of intramolecular rotation, the data obtained will be useful for further studies of the paramagnetic analogues of the synthesized complexes aimed at revealing the correlations between the coordination environment of the lanthanide ions and their magnetic properties.

Experimental

Synthesis of the complexes **[B$_4$]Y[B$_4$]Y[C$_4$]** and $\mathbf{Y_2[B_4]_3}$ was reported previously.[11,12] UV–Vis spectra in the range of 250–900 nm were measured using a JASCO V-770 spectrophotometer in quartz cells with 0.5-1 cm optical path. NMR spectra were recorded on a Bruker Avance III spectrometer with 600 MHz proton frequency at the required temperature with the use of the residual solvent resonances as internal references (dichloromethane 5.32 ppm). Spectra were assigned using ^{1}H-^{1}H COSY, NOESY and ^{1}H-^{13}C HSQC.

Homoleptic complex ***Y$_2$[B$_4$]$_3$***: ^{1}H NMR (600 MHz, dichloromethane-d_2, 303 K) δ 8.37 (s, 8H, H_{Pc}^{i}), 8.00 (s, 16H, H_{Pc}^{o}), 4.89 (q, J = 6.0 Hz, 16H, 1^{i}), 4.62 (q, J = 6.4 Hz, 16H, 1^{o}), 4.32 (q, J = 6.6 Hz, 16H, $1^{o'}$), 2.55 (m, 16H, 2^{i}), 2.17 (m, 48H, 3^{i} and 2^{o}), 1.83 (m, 32H, 3^{o}), 1.54 (t, J = 7.3 Hz, 24H, CH_3^{i}), 1.23 (t, J = 7.3 Hz, 48H, CH_3^{o}).

Heteroleptic complex ***[B$_4$]Y[B$_4$]Y[C$_4$]$_3$:*** ^{1}H NMR (600 MHz, dichloromethane-d_2, 293 K) δ 8.41 (s, 8H, bH_{Pc}^{i}), 7.97 (s, 8H, cH_{Pc}^{o}), 7.84 (s, 8H, bH_{Pc}^{o}), 4.95 (q, J = 5.5 Hz, 8H, 1^{ic}), 4.77 (q, J = 6.0 Hz, 8H, 1^{ib}), 4.65 (q, J = 5.8 Hz, 8H, 1^{o}), 4.59 (t, J = 7.9 Hz, 8H, α^{o}), 4.38 (br s, 8H, $\alpha^{o'}$), 4.27 (q, J = 6.2 Hz, 8H, $1^{o'}$), 3.99 (m, 16H, $\beta^{o,o'}$), 4.02–3.50 (br m, 32H, $\gamma^{o,o'}$ and $\delta^{o,o'}$), 2.49 (m, 16H, 2^{i}), 2.13 (m, 32H, $3^{i}$and 2^{o}), 1.78 (m, 16H, 3^{i}), 1.46 (t, J = 7.3 Hz, 24H, CH_3^{i}), 1.19 (t, J = 7.3 Hz, 24H, CH_3^{o}).

Acknowledgements. The authors acknowledge the financial support from the Russian Science Foundation (no. 18-73-10174-P, https://www.rscf.ru/en/project/21-73-03031/). NMR spectra were measured using the equipment of CKP FMI IPCE RAS.

References

1. Dattler D., Fuks G., Heiser J., Moulin E., Perrot A., Yao X., Giuseppone N. *Chem. Rev.* **2020**, 120, 310–433. DOI:10.1021/acs.chemrev.9b00288.
2. Yao B., Sun H., Yang L., Wang S., Liu X. *Front. Chem.* **2022**, *9*, 832735. DOI:10.3389/fchem.2021.832735.
3. Gisbert Y., Abid S., Kammerer C., Rapenne G. *Chem. – A Eur. J.* **2021**, *27*, 12019–12031. DOI:10.1002/chem.202101489.
4. Martynov A.G., Safonova E.A., Tsivadze A.Y., Gorbunova Y.G. *Coord. Chem. Rev.* **2019**, *387*, 325–347. DOI:10.1016/j.ccr.2019.02.004.
5. Takeuchi M., Ikeda M., Sugasaki A., Shinkai S. *Acc. Chem. Res.* **2001**, *34*, 865–873. DOI:10.1021/ar0000410.
6. Takeuchi M., Imada T., Shinkai S. *J. Am. Chem. Soc.* **1996**, *118*, 10658–10659. DOI:10.1021/ja961480q.
7. Sugasaki A., Ikeda M., Takeuchi M., Robertson A., Shinkai S. *J. Chem. Soc. Perkin Trans. 1* **1999**, 3259–3264. DOI:10.1039/a904890a.
8. Martynov A.G., Polovkova M.A., Berezhnoy G.S., Sinelshchikova A.A., Khrustalev V.N., Birin K.P., Kirakosyan G.A., Gorbunova Y.G., Tsivadze A.Y. *Inorg. Chem.* **2021**, *60*, 9110–9121. DOI:10.1021/acs.inorgchem.1c01100.

9. Pavlov A.A. *INEOS OPEN* **2020**, *2*, 153–162. DOI:10.32931/io1922r.
10. Martynov A.G., Horii Y., Katoh K., Bian Y., Jiang J., Yamashita M., Gorbunova Y.G. *Chem. Soc. Rev.* **2022**, *51*, 9262–9339. DOI:10.1039/d2cs00559j.
11. Martynov A.G., Sinelshchikova A.A., Dorovatovskii P.V., Polovkova M.A., Ovchenkova A.E., Birin K.P., Kirakosyan G.A., Gorbunova Y.G., Tsivadze A.Y. *Inorg. Chem.* **2023**, *62*, 10329–10342. DOI: 10.1021/acs.inorgchem.3c01169.
12. Martynov A.G., Polovkova M.A., Gorbunova Y.G., Tsivadze A.Y. *Molecules* **2022**, *27*, 6498. DOI:10.3390/molecules27196498.
13. Martynov A.G., Yagodin A.V., Birin K.P., Gorbunova Y.G., Tsivadze A.Y. *J. Porphyrins Phthalocyanines* **2023**, 27, 414–422. DOI:10.1142/S1088424623500104.
14. Dobeš P., Řezáč J., Fanfrlík J., Otyepka M., Hobza P. *J. Phys. Chem. B* **2011**, *115*, 8581–8589. DOI:10.1021/jp202149z.
15. Stewart J.J.P. *MOPAC2016 (Molecular Orbital Package). http//openmopac.net/MOPAC2016.html*
16. Ditchfield R. *Mol. Phys.* **1974**, *27*, 789–807. DOI:10.1080/00268977400100711.
17. Neese F. *WIREs Comput. Mol. Sci.* **2022**, 1–15. DOI:10.1002/wcms.1606.
18. Schattenberg C.J., Kaupp M. *J. Chem. Theory Comput* **2021**, *17*, 7602–7621. DOI:10.1021/acs.jctc.1c00919.
19. Jensen F. *J. Chem. Theory Comput.* **2015**, *11*, 132–138. DOI:10.1021/ct5009526.
20. Weigend F. *Phys. Chem. Chem. Phys.* **2006**, *8*, 1057–1065. DOI:10.1039/b515623h.
21. Hay P.J., Wadt W.R. *J. Chem. Phys.* **1985**, *82*, 270–283. DOI:10.1063/1.448799.
22. Pople J.A. *High Resolution Nuclear Magnetic Resonance*, **1959**.
23. Anet F.A.L., Bourn A.J.R. *J. Am. Chem. Soc.* **1967**, *89*, 760–768. DOI:10.1021/ja00980a006.
24. Gutowsky H.S., Cheng H.N. *J. Chem. Phys.* **1975**, *63*, 2439–2441. DOI:10.1063/1.431673.
25. Kleinwächter J., Hanack M. *J. Am. Chem. Soc.* **1997**, *119*, 10684–10695. DOI:10.1021/ja962663f.
26. Katoh K., Kajiwara T., Nakano M., Nakazawa Y., Wernsdorfer W., Ishikawa N., Breedlove B. K., Yamashita M. *Chem. - A Eur. J.* **2011**, *17*, 117–122. DOI:10.1002/chem.201002026.
27. Horii Y., Katoh K., Miyazaki Y., Damjanović M., Sato T., Ungur L., Chibotaru L.F., Breedlove B.K., Nakano M., Wernsdorfer W., Yamashita M. *Chem. - A Eur. J.* **2020**, *26*, 8076–8082. DOI:10.1002/chem.201905796.

Received 25.04.2023
Accepted 10.06.2023